Cloning, characterization, and expression features of chicken CDS2 splicing variants

Yuanyuan Xu
Henan Agricultural University
Shuping Zhang
Henan Agricultural University
Yujun Guo
Henan Agricultural University
Wen Chen
Henan Agricultural University
Yanqun Huang (hyanqun@aliyun.com)
Henan Agricultural University

Research Article

Keywords: chicken, CDS2, transcript variant, gene expression, insulin

Posted Date: September 29th, 2020

DOI: https://doi.org/10.21203/rs.3.rs-84009/v1

Abstract

Background: The CDS gene encodes the CDP-diacylglycerol synthase enzyme that catalyzes the formation of CDP-diacylglycerol (CDP-DAG) from phosphatidic acid. At present, there are no reports of CDS2 in birds. Here, we identified chicken CDS2 transcripts, explored the spatio-temporal expression profiles of total CDS2 and the longest transcript variant CDS2-4, and investigated the effect of exogenous insulin on total the mRNA level of CDS2.

Results: Four transcripts of chicken CDS2 (CDS2-1, -2, -3, and -4) were identified, which were alternatively spliced at the 3'-untranslated region (UTR). Chicken CDS2 was located at chr.22, where there was a chromosomal fusion/break event in the evolution of mammals and birds. CDS2 was widely expressed in all tissues examined and the longest variant CDS2-4 was the major transcript. Both total CDS2 and CDS2-4 were prominently expressed in adipose tissue and the heart, and exhibited low expression in the liver and pectoralis of 49 day-old chickens. Quantitative real-time PCR revealed that total CDS2 and CDS2-4 had different spatio-temporal expression patterns in chicken. Total CDS2 exhibited a similar temporal expression tendancy with a high level in the later period of incubation (embryonic day 19 [E19] or 1-day-old) in the brain, liver, and pectoralis. While CDS2-4 presented a distinct temporal expression pattern in these tissues, CDS2-4 levels peaked at 21 days in the brain and pectoralis, while liver CDS2-4 mRNA levels were highest at the early stage of hatching (E10). Total CDS2 ($P < 0.001$) and CDS2-4 ($P = 0.0090$) mRNA levels in the liver were differentially regulated throughout development of the chicken. Exogenous insulin significantly downregulated the level of total CDS2 at 240 min in the pectoralis of Silky chickens ($P < 0.01$). Total CDS2 levels in the liver of Silky chickens were higher than that of the broiler in the basal state and after insulin stimulation.

Conclusion: Chicken CDS2 has multiple transcripts with variation at the 3'-UTR, which was prominently expressed in adipose tissue. Total CDS2 and CDS2-4 presented distinct spatio-temporal expression patterns, and they were differentially regulated with age in liver. Insulin could regulate chicken CDS2 levels in a breed- and tissue-specific manner.

Background

CDP-diacylglycerol synthases (CDSs) are critical enzymes that catalyze the synthesis of cytidine diphosphate diacylglycerol (CDP-DAG) from phosphatidic acid to produce phospholipids such as phosphatidylinositol, phosphatidylglycerol, and cardiolipin [1, 2]. The gene encoding CDS was first cloned from *Escherichia coli* in 1985 [3], while the first eukaryotic CDS was cloned from *Drosophila* in 1995, which shares 31% amino acid similarity with bacterial CDS [4]. CDS cDNA sequences were subsequently cloned from yeast [5], human [6-9], rat [10], mouse [11, 12], and pig [13]. All eukaryotic genomes have been shown to contain CDS homologs [7, 14, 15] and the number of CDS genes varies in different organisms [16]. There is one CDS gene in yeast and fly [17], and two CDS genes (CDS1 and CDS2) in vertebrates [7], including rat, mice, human, and zebrafish [16].

The expression of mammalian CDS2 is ubiquitous [10-12]. Recent research revealed that CDS is involved in numerous cellular functions. Studies from *Drosophila* highlight the importance of CDS (CdsA) in the visual photo-transduction system [4]. Mutations in the eye-specific CDS gene in *Drosophila* resulted in a defect in photo-transduction and retinal degeneration [4]. CDS also plays an important role in the regulation of vascular endothelial growth factor-A (VEGFA) signaling and angiogenesis [18]. Loss of CDS2 has been shown to cause a defect in VEGF signaling activity and angiogenic capacity in zebrafish, primarily by decreasing the level of PIP2 regeneration [19]. Genetic ablation of CDS2 switches the output of VEGFA signaling from promoting angiogenesis to inducing vessel regression and tumor inhibition [18]. Recent reports have revealed that the CDS gene is involved in lipid metabolism [1, 2, 15, 20, 21], and mammalian CDS1 and CDS2 regulate lipid droplets through distinct mechanisms [21]. Human CDS1 and CDS2 can create different CDP-DAG pools; CDS2 is selective for acyl chains at the sn-1 and sn-2 positions [22]. The importance of CDS enzymes stems from the need for cells to maintain their phosphoinositide levels, in particular, those of PIP2 [7, 16].

Although Tam41 also catalyzes the synthesis of CDP-DAG using phosphatidic acid and cytidine 5'-triphosphate as substrates, it shares no sequence or structural homology with the CDS enzyme [17, 23]. In addition, CDS is an integral membrane protein, whilst Tam41 is a peripheral membrane protein [14, 17, 23].

Until now, there have been no reports of a CDS gene in birds. In this study, we identified chicken CDS2 transcripts, analyzed the genomic structure, chromosomal synteny, spatio-temporal expression pattern, and the effect of exogenous insulin on chicken CDS2, revealing the basic characteristics of chicken CDS2 and further identifying the function of CDS2 in the regulation of chicken development and growth.

Results

Cloning and identification of chicken CDS2 splice variants

Based on the predicted chicken CDS2 sequence (XM_417669), four CDS2 transcripts alternatively spliced at the 3'-untranslated region (UTR) were cloned by combining conventional PCR amplification (LP1–LP5, Fig. S1), 5' RACE (Fig. 1A), and 3' RACE (Fig. 1B) and named CDS2-1 (4643 bp, GenBank accession no. KC886604), CDS2-2 (4770 bp, GenBank accession no. KC886602), CDS2-3 (4893 bp, GenBank accession no. KC886601), and CDS2-4 (5545 bp, GenBank accession no. KC886603). The sequence of the longest transcript CDS2-4 was consistent with the predicted CDS2 (accession no. XM_417669). Cloned CDS2 transcripts containing part of the 5'-UTR, 1348 bp coding sequence, and a long 3'-UTR ranged from 3265 to 4167 bp with a polyA signal (AATAAA) and polyA tail, with differences at 4310–5210 bp compared with the longest transcript CDS2-4, and were predicted to encode proteins of 448 amino acids. The sequence in the alternative region of chicken CDS2 was predicted to contain multiple binding sites of microRNA (miRNA) sequences including gga-miR-12243-5p and gga-miR-12215-5p (http://www.mirbase.org/search.shtml), as well as gga-miR-1680-5p, gga-miR-1751-5p, gga-miR-301b-5p, and gga-miR-6561-3p (http://www.mirdb.org/custom.html).

Chicken CDS2 is located at chr.22, spanning approximately 23 kb of the genome (Table S1). The longest splice form (CDS2-4) contains 13 exons with the exon–intron boundary (Table S1) abiding by the GT-AG rule; while CDS2-1, CDS2-2, and CDS2-3 contain 14 exons. The exon–intron boundary of intron 13 abides by AC-AG for CDS2-3, GC-CA for CDS2-2, and CT-AG for CDS2-1 (http://genome.ucsc.edu/cgi-bin/hgBlat, Table S1).

Conservation of CDS2 sequences among species

We investigated the sequence similarity of the coding sequence, predicted AA sequence, and the 3'-UTR of CDS2 among species. The chicken CDS2 coding sequence shared 96% similarity with turkey (XM_021375090.1), 81.0% with human (NM_003818.3), 81.2% with mouse (NM_138651.6), 81.1% with cattle (NM_001078046.1), 76.5% with frog (NM_001126503.1), and 78.7% with zebrafish (NM_201186.1). The deduced amino acid sequence of chicken CDS2 shared 99.1% homology with turkey (XP_010721376.1), 91.4% with human (NP_003809.1), 93.0% with mouse (NP_619592.1), 91.0% with cattle (NP_001071514.1), 85.9% with zebrafish (NP_957480.1), and 87.7% with frog (NP_001119975.1) (Fig. S2). The 3'-UTR sequence of chicken CDS2 (KC886603) was also conserved among birds, which shares 87.7% identity with quail (NC_029537.1), 75.3% with duck (NC_045585.1), and 75.2% with goose (NW_013185922.1). The 3'-UTR of CDS2 among mammals was also conserved and the 3'-UTR of CDS2 in humans (NM_003818.3) shared more than 93% similarity with monkey (XM_012052138.1), 71.7% with horse (XM_005604492.3), and 67.6% with seal (XM_027118224.1) while no identical sequences were identified in the 3'-UTR of CDS2 between birds and mammals.

Syntenic analysis revealed that chicken CDS2 was located between PCNA and ARHGAP25/BMP10 on chr.22, close to the chromosomal breakage/fusion point of the mammalian/bird evolutionary event. The upstream chromosomal region of CDS2 in birds containing the CDS2-PCNA-TMEM230-SVCT gene is homologous to chr.20 in human and chr.2 in mouse while the downstream chromosomal region containing ARHGAP25-BMP10-GKN2-GKN1 was homologous to chr.2 in human and chr.6 in mouse (Fig. 2). The amino acid phylogenetic tree of CDS2 (Fig. S3) reflects the evolutionary relationship among species similar to the syntenic analysis of chromosomes (Fig. 2).

Tissue expression profile of chicken CDS2

We conducted semi-quantitative reverse transcription PCR (RT-PCR) and qPCR to investigate the tissue expression pattern of chicken CDS2 in 49 day-old Silky chickens with CP2, AS1, and QP2 primer sets (Table S2).

Amplification with the CP2 primer set located in the coding region of the CDS2 gene reflects the total expression level of CDS2 (referred to as total CDS2). Total CDS2 was extensively expressed in all detected tissues (Fig. 3A). The qPCR revealed that total CDS2 was relatively highly expressed in adipose tissues including sebum (at the tail root), abdominal fat, and neck fat, followed by heart and leg muscle, and weakly expressed in the liver and pectoralis (P = 0.0528, Fig. 3B).

Primer pair AS1, which can simultaneously amplify four splicing forms, was used to observe the tissue expression pattern of multiple transcripts by semi-quantitative RT-PCR (Figs. 4A and S4). The amplified lengths of the CDS2-1, CDS2-2, CDS2-3, and CDS2-4 transcripts should be 245, 379, 504, and 1142 bp, respectively. QP2 is located in the specific region of the longest transcript CDS2-4, which could specifically detect expression of the CDS2-4 variant. CDS2-4 was extensively expressed, and predominantly present in nearly all detected tissues (Figs. 4 and S4). Expression of CDS2-3 was detected in almost all tissues, while the short transcripts CDS2-1 and CDS2-2 were undetected with the AS1 primer set in two separate experiments (Figs. 4A and S4).

The qPCR with the QP2 primer revealed that CDS2-4 showed a similar expression pattern as total CDS2, with a relative high mRNA level in adipose tissues including sebum, abdominal fat, and neck fat, followed by heart, testis, brain, and leg muscle, and low levels in the liver and pectoralis (Fig. 5). Compared with the tissue expression pattern of total CDS2 detected with the CP2 primer set ($P = 0.0528$, Fig. 3B), the level of CDS2-4 showed greater tissue fluctuation ($P < 0.0001$, Fig. 5). CDS2-4 exhibited similar mRNA levels in heart and adipose tissues including sebum, abdominal fat, and neck fat, while CDS2-4 levels in abdominal fat were significantly higher than those of other tissues ($P < 0.01$). The CDS2-4 level in adipose tissue was approximately four-fold that in the testis and 120-fold that in the liver (Fig. 5).

The spatio-temporal expression patterns of total CDS2 and CDS2-4

We further investigated the spatio-temporal expression patterns of total CDS2 (with the CP2 primer set) and CDS2-4 (with the QP2 primer set) by qPCR. One-way ANOVA was used to analyze the effect of age and tissue on the expression of total CDS2 and CDS2-4 separately. Total CDS2 exhibited similar temporal expression patterns (Fig. 6A) in the brain ($P = 0.1623$), liver ($P < 0.0001$), and pectoralis ($P = 0.1712$). In general, the total CDS2 mRNA level was the highest in the later stage of embryogenesis (embryonic day 19 [E19]/ one-day-old [D1]), and the E19 level in the liver was significantly higher than that of the other time points ($P < 0.05$). In addition, the relative expression of total CDS2 in the brain was significantly ($P < 0.05$) higher than that in the liver (9-fold) and pectoralis (3-fold) at 49 days (Fig. 6A).

Unlike total CDS2, the mRNA level of the CDS2-4 variant presented a distinct temporal change in pattern in the brain, liver, and pectoralis (Fig. 6B). CDS2-4 levels peaked at 21 days in the brain ($P = 0.1336$) and pectoralis ($P = 0.0104$). The level of CDS2-4 in the pectoralis at 21 days was significantly higher than that at the other ages tested, with the exception of 1 day ($P < 0.05$); whereas hepatic CDS2-4 levels presented a decreasing trend with development, with highest levels at the early stage of hatching (E10), a weak decrease during embryogenesis (E14–D1), and a clear decrease with age after hatching (D21 and D49, $P = 0.009$). Hepatic CDS2-4 levels at E10 were significantly higher than at 21 days ($P < 0.05$) and 49 days ($P < 0.01$) (Fig. 6B). In addition, the brain had the highest level of CDS2-4 at all time points among the three tissues; brain CDS2-4 levels at 21 days were significantly higher than those in the liver and pectoralis ($P < 0.01$, Fig. 6B).

Effect of exogenous insulin on chicken CDS2 expression

Exogenous insulin resulted to the rapid drop of blood glucose (until 120min) in both Silky chickens and broilers, and Silky chickens presented a more rapid recovery of blood glucose than broilers after 120 min (Fig. 7A and 7B). Exogenous insulin downregulated the expression of total CDS2 in the pectoralis of Silky fowl ($p = 0.003$, Fig. 7F), where the total CDS2 level at 240 min was significantly lower than at 0 and 120 min (Fig. 7F), and the total CDS2 level in the pectoralis of Silky chickens was lower than that of broiler chickens at 240 min after insulin injection ($P < 0.05$, Fig. 7H). The mRNA level of total CDS2 in the liver of Silky chickens was higher than that of broilers at the basal state and after insulin stimulation ($P < 0.05$, Fig. 7G), and exogenous insulin could weakly upregulate the mRNA level of total CDS2 at 240 min in the livers of broilers ($P = 0.078$, Fig. 7C).

Discussion

Four transcripts of chicken CDS2 (CDS2-1–4) were identified; the transcripts were alternatively spliced at the 3'-UTR. Consistent with the 3'-RACE results (Fig. 1B), the longest product CDS2-4 was the major transcript observed using RT-PCR (with AS1 primers), while only two long transcript variants (CDS2-3 and CDS2-4) were detected from multiple tissues in two separate experiments (Figs. 4A and S4). The differences in identified transcript types may be because RACE technology is more sensitive than conventional RT-PCR. We also observed that the expression level of CDS2-3 was similar to that of CDS2-4 in the small intestine, kidney, brain, and abdominal fat tissues of one Silky chicken (Fig. 3A), but was weak in nearly all detected tissues of another individual (Fig. S4), suggesting that the expression of CDS2-3 varied greatly among individuals/tissues and the function of CDS2-3 needs to be further clarified.

3'-UTRs are major players in gene regulation that enable local function, compartmentalization, and cooperativity [24]. Birds and mammals share high sequence similarity for the deduced CDS2 proteins, while possessing their own conservative 3'-UTR, suggesting that the 3'-UTR of CDS2 may play an important role in regulating the phenotypic diversity of higher organisms [24]. The average length of 3'-UTRs in human are 1278 nt [25]; CDS2 exhibited a long 3'-UTR both in mammals (9000 nt in human) and birds (5210 nt in chicken), suggesting there may be an abundance of regulatory elements in the 3'-UTR of CDS2. The shortening/lengthening of the 3'-UTR may result in a change in miRNA binding sites [26]. Further studies are needed to confirm the relationship between these miRNAs and CDS2.

CDS has been linked with lipid metabolism [1, 2, 15, 20, 21], with a stronger effect on phosphatidic acid levels. CDS2 deficiency (while not CDS1) could impair the maturation of initial lipid droplets in cultured mammalian cells [21]. A transcriptome profile revealed that CDS2 was differentially expressed in adipose tissues of fat- and short-tailed Chinese sheep [27]. Here, we observed that chicken CDS2 was predominantly expressed in multiple adipose tissues, which provide direct evidence for a function of CDS2 in fat metabolism.

The level of CDS2 was low in chicken livers at 49 days, but mRNA levels of CDS2 showed dramatic changes during development. Livers in birds play a central role in lipid metabolism, serving as the center for lipoprotein uptake, formation, and export to the circulation [28, 29], while adipose tissue functions

primarily as a storage tissue [30]. Zhao et al. reported that hepatic triglyceride levels increased during embryonic development [31, 32]. While post-hatching, the liver lipid content correlated negatively with broiler age; it was the highest on the first day then decreased sharply at day 7 [29, 33]. Here, we observed that total CDS2 mRNA exhibited a similar temporal change pattern as hepatic lipids during development. The changes in lipid and gene expression of the liver were indicative of the rapid alteration of the role of the liver in lipid metabolism during development. In addition, it has been reported that the serum lipid level (total cholesterol and triglyceride) of Silky chickens was higher than that of broilers [34]. Here, we found that total CDS2 levels in livers of Silky chickens were twice that of broilers at 47 days, which suggested that CDS2 contributes to lipid metabolism.

In past work, our group found a 30% energy restriction in broiler chickens significantly reduced the abdominal fat ratio and subcutaneous fat thickness [35], and downregulated an unknown differentially expressed fragment C7-2 (mapped to chicken EST CR406381.1) [36] in broiler's liver tissue. With the update of the chicken genomic database in NCBI, this fragment has now been mapped to the 3'-UTR of chicken CDS2 (XM_004947552). The downregulation of CDS2 in chicken liver by energy restriction demonstrated the association of chicken CDS2 with fat metabolism.

It has been reported that Silky chickens exhibit a stronger ability to regulate glucose homeostasis than broilers under exogenous insulin stimulation. Silky chickens showed a greater blood glucose recovery than broilers at 240 min regardless of whether food was served at 120 min after insulin stimulation [34, 37]. Skeletal muscles have been considered a major regulator of systemic glucose homeostasis [38]. Here, exogenous insulin significantly downregulated the level of total CDS2 at 240 min in the pectoralis of Silky chickens, which reflects the involvement of CDS2 in the insulin signaling pathway in a breed- and tissue-specific manner. Loss of CDS in *Drosophila* has been reported to cause a decrease in phosphatidylinositol and insulin signaling [1].

Conclusion

In summary, four alternatively spliced forms of CDS2 with variations at the 3'-UTR were identified in chicken, and the longest form, CDS2-4, was the main transcript. Both total CDS2 and CDS2-4 were extensively expressed in all detected tissues, and predominantly present in adipose tissues including sebum, abdominal fat, and neck fat. Total CDS2 and CDS2-4 presented distinct spatio-temporal expression patterns in the brain, liver, and pectoralis during chicken development. Total hepatic CDS2 and CDS2-4 were dramatically regulated with age in a distinctly different manner. Total CDS2 in the liver of Silky chickens was significantly higher than that of broilers at the basal state and after insulin stimulation. Total CDS2 in the pectoralis of Silky chickens was insulin sensitive; this level was significantly downregulated at 240 min after exogenous insulin stimulation.

Methods

Sample collection

Chickens and fertilized eggs were obtained from the poultry germplasm resources farm of Henan Agricultural University. The one-day-old Arbor Acres (AA) broilers and Silky chickens were cage raised routinely until 49 days with free access to food and water as described previously [34]. The diet was prepared based on nutritional standards for broilers recommended by the NRC (Nutrient Requirements for Poultry, 1994). The fertilized eggs from the Silky population were collected and hatched under conventional conditions. The research protocol was approved by the Animal Care and Use Committee of Henan Agricultural University (Zhengzhou, China).

To identify the spatio-temporal characteristics of chicken CDS2 transcripts, brain, liver, and pectoralis tissues were collected from Silky chickens at E10, E15, E19, one-day-old (newly hatched birds, D1), D21, and D49 (n = 3 for each time point). The samples were snap-frozen immediately in liquid nitrogen and stored at -80℃ for RNA isolation.

To investigate the effect of exogenous insulin on CDS2 mRNA expression, at 47 days (after 12 h fasting), female AA broilers (average weight, 1.86 kg, n = 12) and Silky fowls (average weight, 0.75 kg, n = 12) were randomly selected and administered an insulin tolerance test (with hypodermic injection of 80 μg/kg body weight insulin or equal PBS solution as the control) as described previously [34], and birds were given feed at 120 min. The fowls were sacrificed at 0 min (before insulin injection), 120 min, and 240 min after insulin injection (5–6 birds/breed at each time point). All chickens were euthanized by cervical dislocation prior to tissue isolation. The pectoralis and liver were collected and snap-frozen immediately in liquid nitrogen and stored at -80℃ for RNA isolation.

RNA extraction and first-strand complementary DNA (cDNA) synthesis

Total RNA was extracted from tissues according to the manufacturer's instructions (RNAiso Plus, TaKaRa, Dalian, China). The quality and concentration of the extracted RNA was determined by agarose gel electrophoresis and a spectrophotometer (Thermo NanoDrop One, DE, USA) respectively. The RNA was then reverse-transcribed using a PrimeScript™ RT reagent Kit with gDNA Eraser (TaKaRa) in a 20 μl reaction containing 1 μg of total RNA and random primers. The synthesized cDNA samples were stored at -20°C.

Identification of CDS2 transcripts

CDS2 transcripts were identified by combining conventional RT-PCR amplification, and 5' and 3' rapid amplification of cDNA ends (RACE). The primers for amplifying the CDS2 gene were designed based on the sequence of EST CR406381.1 and the predicted chicken CDS2 sequence (accession no. XM_417669.5), and listed in Table S2. CDS2 transcripts were identified from the ovary tissue of Silky chickens.

5' and 3' RACE were used to identify CDS2 transcripts using the SMART^{TM} RACE cDNA Amplification Kit (Clontech Laboratories Inc., CA, USA) according to the manufacturer's instructions. PCR was conducted in a total volume of 50 μl, containing 2.5 μl 5' or 3'-ready cDNA, 1.0 μl GSP1 or GSP2 primer (10 μM), 2.5 μl

UPM (10 μM), and 41.5 μl Master Mix and was performed according to a touchdown PCR protocol: five cycles of amplification (94℃ for 30 s and 72℃ for 3 min) followed by five cycles of 94℃ for 30 s, 70℃ for 30 s, and 72℃ for 3 min, and 25 cycles of 94℃ for 30 s, 68℃ for 30 s, and 72℃ for 3 min. The amplified products for 5'- and 3'-RACE were purified and cloned into the pMD-18T vector (TaKaRa), and transformed into *E. coli* DH5α. In addition, 6–10 positive clones were confirmed by Sanger sequencing.

Quantitative real-time PCR (qPCR)

qPCR was carried out with a CFX96™ Real-Time PCR Detection Systems (Bio-Rad Laboratories, Hercules, CA, USA) using 2× M5 HiPer Dual Real-time PCR Super Mix (SYBRgreen with anti-Taq, Mei5bio). The β-actin gene was used as an internal control. The primers for qPCR (Table S2) were optimized as previously described [39]. PCR amplification was performed in a total volume of 10 μl containing 5 μl Real-time PCR Super Mix (SYBRgreen with anti-Taq, Mei5bio), 1.0 μl cDNA, and 0.25 μmol/L of forward and reverse primer as follows: 95℃ for 5 min, followed by 40 cycles of 95℃ for 10 s, 60℃ for 15 s, and 72℃ for 30 s, and a final incubation at 72℃ for 10 min, followed by a final 5 min extension at 72°C. Three technical replicates were performed for each sample. Relative gene expression was calculated using the $2^{-\Delta\Delta Ct}$ method [7].

Bioinformatics analysis

CDS2 sequence similarity was compared with the NCBI database (https://www.ncbi.nlm.nih.gov/). The genomic structure of chicken CDS2 was analyzed with the UCSC Genome Browser (http://genome.ucsc.edu/cgi-bin/hgBlat). PhyloView in Genomicus v100.01 was used to analyze the consensus conserved genomic synteny of CDS2 (https://www.genomicus.biologie.ens.fr/genomicus-100.01/cgi-bin/search.pl). Amino acid sequence alignment was performed using ClustalW software. A neighbor-joining phylogenetic tree was constructed based on aligned amino acid sequence using MEGA 6.0, and edited by the tree view program with a bootstrap value of 1000. Alternative splicing of potential miRNA binding sites was predicted using the databases miRDB (http://www.mirdb.org/custom.html) and miRBase (http://www.mirbase.org/ search.shtml).

Statistical analysis

Data were analyzed by one-way analysis of variance using IBM SPSS Statistics 22.0 software and expressed as mean ± standard error. Multiple comparisons were conducted using the Bonferroni method. GraphPad Prism 5.0 software was used to prepare graphs. $P < 0.05$ was considered significant and $P < 0.01$ was considered extremely significant.

Declarations

Acknowledgments

Not applicable.

Authors' contributions

XYY, CW, and HYQ conceived and designed the experiments. XYY, GYJ, and ZSP performed the experiments. XYY, ZSP, and CW analyzed the data. XYY and HYQ wrote the manuscript. All authors read and approved the final manuscript.

Funding

This research was supported by the National Natural Science Foundation of China (32072748). The funding bodies had no role in study design or in any aspect of the collection, analysis and interpretation of data or in writing the manuscript.

Availability of data and materials

All data generated and analyzed during this study are included in this published article.

Ethics approval and consent to participate

The hatched fertilized eggs and chickens were from the poultry germplasm resources farm of Henan Agricultural University. The research protocol was approved by the Animal Care and Use Committee of Henan Agricultural University (Zhengzhou, China).

Consent for publication

Not applicable.

Competing interests

The authors declare that they have no competing interests.

Abbreviations

CDS, CDP-diacylglycerol synthase; CDP-DAG, cytidine diphosphate diacylglycerol; VEGFA, vascular endothelial growth factor-A; E10, embryonic day 10; D1, one-day-old; RACE, rapid amplification of cDNA ends; RT-PCR, reverse transcription PCR; qPCR, quantitative real-time PCR; 3'-UTR, 3'-untranslated region.

References

1. Liu Y, Wang W, Shui G, Huang X. CDP-diacylglycerol synthetase coordinates cell growth and fat storage through phosphatidylinositol metabolism and the insulin pathway. PLoS Genet. 2014; 10(3):e1004172.
2. Qi Y, Kapterian T, Du X, Ma Q, Fei W, Zhang Y, Huang X, Dawes I, Yang H. CDP-diacylglycerol synthases regulate the growth of lipid droplets and adipocyte development. J Lipid Res. 2016; 57(5):767-780.

3. Icho T, Sparrow CP, Raetz CR. Molecular cloning and sequencing of the gene for CDP-diglyceride synthetase of Escherichia coli. J Biol Chem. 1985; 260(22):12078-12083.
4. Wu L, Niemeyer B, Colley N, Socolich M, Zuker CS. Regulation of PLC-mediated signalling in vivo by CDP-diacylglycerol synthase. Nature. 1995; 373(6511):216-222.
5. Shen H, Heacock PN, Clancey CJ, Dowhan W. The CDS1 gene encoding CDP-diacylglycerol synthase in Saccharomyces cerevisiae is essential for cell growth. J Biol Chem. 1996; 271(2):789-795.
6. Heacock AM, Uhler MD, Agranoff BW. Cloning of CDP-Diacylglycerol Synthase from a Human Neuronal Cell Line. J Neurochem. 1996; 67(5):2200-2203.
7. Lykidis A, Jackson PD, Rock CO, Jackowski S. The role of CDP-diacylglycerol synthetase and phosphatidylinositol synthase activity levels in the regulation of cellular phosphatidylinositol content. J Biol Chem. 1997; 272(52):33402.
8. Weeks R, Dowhan W, Shen H, Balantac N, Meengs B, Nudelman E, Leung DW. Isolation and expression of an isoform of human CDP-diacylglycerol synthase cDNA. DNA Cell Biol. 1997; 16(3):281-289.
9. Halford S, Dulai KS, Daw SC, Fitzgibbon J, Hunt DM. Isolation and chromosomal localization of two human CDP-diacylglycerol synthase (CDS) genes. Genomics. 1998; 54(1):140-144.
10. Saito S, Goto K, Tonosaki A, Kondo H. Gene cloning and characterization of CDP-diacylglycerol synthase from rat brain. J Biol Chem. 1997; 272(14):9503.
11. Volta M, Bulfone A, Gattuso C, Rossi E, Mariani M, Consalez GG, Zuffardi O, Ballabio A, Banfi S, Franco B. Identification and characterization of CDS2, a mammalian homolog of the Drosophila CDP-diacylglycerol synthase gene. Genomics. 1999; 55(1):68-77.
12. Inglis-Broadgate SL, Ocaka L, Banerjee R, Gaasenbeek M, Chapple JP, Cheetham ME, Clark BJ, Hunt DM, Halford S. Isolation and characterization of murine Cds (CDP-diacylglycerol synthase) 1 and 2. Gene. 2005; 356:19-31.
13. Mercade A, Sanchez A, Folch J. Characterization and physical mapping of the porcine CDS1 and CDS2 genes. Anim Biotechnol. 2007; 18(1):23-35.
14. Blunsom NJ, Gomez-Espinosa E, Ashlin TG, Cockcroft S. Mitochondrial CDP-diacylglycerol synthase activity is due to the peripheral protein, TAMM41 and not due to the integral membrane protein, CDP-diacylglycerol synthase 1. BBA-Mol Cell Biol L. 2018; 1863(3):284-298.
15. Kong P, Ufermann CM, Zimmermann DLM, Yin Q, Suo X, Helms JB, Brouwers JF, Gupta N. Two phylogenetically and compartmentally distinct CDP-diacylglycerol synthases cooperate for lipid biogenesis in Toxoplasma gondii. J Biol Chem. 2017; 292(17):7145-7159.
16. Blunsom NJ, Cockcroft S. CDP-Diacylglycerol Synthases (CDS): Gateway to Phosphatidylinositol and Cardiolipin Synthesis. Front Cell Dev Biol. 2020; 8:63.
17. Liu X, Yin Y, Wu J, Liu Z. Structure and mechanism of an intramembrane liponucleotide synthetase central for phospholipid biosynthesis. Nat Commun. 2014; 5:4244.

18. Zhao W, Cao L, Ying H, Zhang W, Li D, Zhu X, Xue W, Wu S, Cao M, Fu C *et al*. Endothelial CDS2 deficiency causes VEGFA-mediated vascular regression and tumor inhibition. Cell Res. 2019; 29(11):895-910.
19. Pan W, Pham VN, Stratman AN, Castranova D, Kamei M, Kidd KR, Lo BD, Shaw KM, Torres-Vazquez J, Mikelis CM *et al*. CDP-diacylglycerol synthetase-controlled phosphoinositide availability limits VEGFA signaling and vascular morphogenesis. Blood. 2012; 120(2):489-498.
20. Qi Y, Sun L, Yang H. Lipid droplet growth and adipocyte development: mechanistically distinct processes connected by phospholipids. BBA-Mol Cell Biol L. 2017; 1862(10 Pt B):1273-1283.
21. Xu Y, Mak HY, Lukmantara I, Li YE, Hoehn KL, Huang X, Du X, Yang H. CDP-DAG synthase 1 and 2 regulate lipid droplet growth through distinct mechanisms. J Biol Chem. 2019; 294(45):16740-16755.
22. D'Souza K, Kim YJ, Balla T, Epand RM. Distinct properties of the two isoforms of CDP-diacylglycerol synthase. Biochemistry. 2014; 53(47):7358-7367.
23. Jiao H, Yin Y, Liu Z. Structures of the Mitochondrial CDP-DAG Synthase Tam41 Suggest a Potential Lipid Substrate Pathway from Membrane to the Active Site. Structure. 2019; 27(8):1258-1269.e1254.
24. Mayr C. Regulation by 3 -Untranslated Regions. Annu Rev Genet. 2017; 51:171–194.
25. Zhao W, Blagev D, Pollac JLk, Erle DJ. Toward a Systematic Understanding of mRNA 3' Untranslated Regions. Proc Am Thorac Soc. 2011; 8: 163–166.
26. Yuan F, Hankey W, Wagner EJ, Li W, Wang Q. Alternative polyadenylation of mRNA and its role in cancer. Genes Dis. 2019; https://doi.org/10.1016/j.gendis.2019.10.011.
27. Wang X, Zhou G, Xu X, Geng R, Zhou J, Yang Y, Yang Z, Chen Y. Transcriptome profile analysis of adipose tissues from fat and short-tailed sheep. Gene. 2014; 549(2):252-257.
28. Arvind A, Osganian SA, Cohen DE, Corey KE. Lipid and Lipoprotein Metabolism in Liver Disease. In: *Endotext.* Edited by Feingold KR, Anawalt B, Boyce A, Chrousos G, Dungan K, Grossman A, Hershman JM, Kaltsas G, Koch C, Kopp P *et al*. South Dartmouth (MA): MDText.com, Inc. Copyright © 2000-2020, MDText.com, Inc.; 2000.
29. Alshamy Z, Richardson KC, Harash G, Hünigen H, Röhe I, Hafez HM, Plendl J, Al Masri S. Structure and age-dependent growth of the chicken liver together with liver fat quantification: A comparison between a dual-purpose and a broiler chicken line. PLoS One. 2019; 14(12):e0226903.
30. Na W, Wu YY, Gong PF, Wu CY, Cheng BH, Wang YX, Wang N, Du ZQ, Li H. Embryonic transcriptome and proteome analyses on hepatic lipid metabolism in chickens divergently selected for abdominal fat content. BMC Genomics. 2018; 19(1):384.
31. Zhao S, Ma H, Zou S, Chen W, Zhao R. Hepatic lipogenesis in broiler chickens with different fat deposition during embryonic development. J Vet Med A Physiol Pathol Clin Med. 2007; 54(1):1-6.
32. Gomez MA, Rodriguez FC. A Study of the Hepatic Lipids during Chick Embryo Development Effect of Triiodothyronine. Exp Clin Endocrinol Diabetes. 1987; 90(2):249-252.
33. Noble RC, Ogunyemi D. Lipid Changes in the Residual Yolk and Liver of the Chick Immediately after Hatching. Biol Neonate. 1989; 56(4):228-236.

34. Ji JF, Tao YF, Zhang XL, Pan JJ, ZHu XH, Wang HJ, Du PF, Zhu Y, Huang YQ, Chen W. Dynamic changes of blood glucose, serum biochemical parameters and gene expression in response to exogenous insulin in Arbor Acres broilers and Silky fowls. Sci Rep. 2020; 10:6697
35. Chen W, Guo YM, Huang YQ, Shi YH, Zhang CX, Wang JW. Effect of Energy Restriction on Growth, Slaughter Performance, Serum Biochemical Parameters and Lpin2/WDTC1 mRNA Expression of Broilers in the Later Phase. J Poult Sci. 2012; 49:12-19.
36. Wang J, Chen W, Kang X, Huang Y, Tian Y, Wang Y. Identification of differentially expressed genes induced by energy restriction using annealing control primer system from the liver and adipose tissues of broilers. Poult Sci. 2012; 91(4):972-978.
37. Wang H, Du P, Zhang J, Zhu Y, Ji J, Chen W, Y H. Effects of exogenous insulin injection on blood glucose metabolism and feeding status in different breed of chicken. Chin J Anim Nutr (in Chinese). 2020; 32(2164-2162).
38. Honka MJ, Latva-Rasku A, Bucci M, Virtanen KA, Nuutila P. Insulin Stimulated Glucose Uptake in Skeletal Muscle, Adipose Tissue and Liver: A Positron Emission Tomography Study. Eur J Endocrinol. 2018; 178(5):523-531.
39. Bustin S. Quantification of mRNA using real-time reverse transcription PCR (RT-PCR): trends and problems. J Mol Endocrinol. 2002; 29(1):23.

Figures

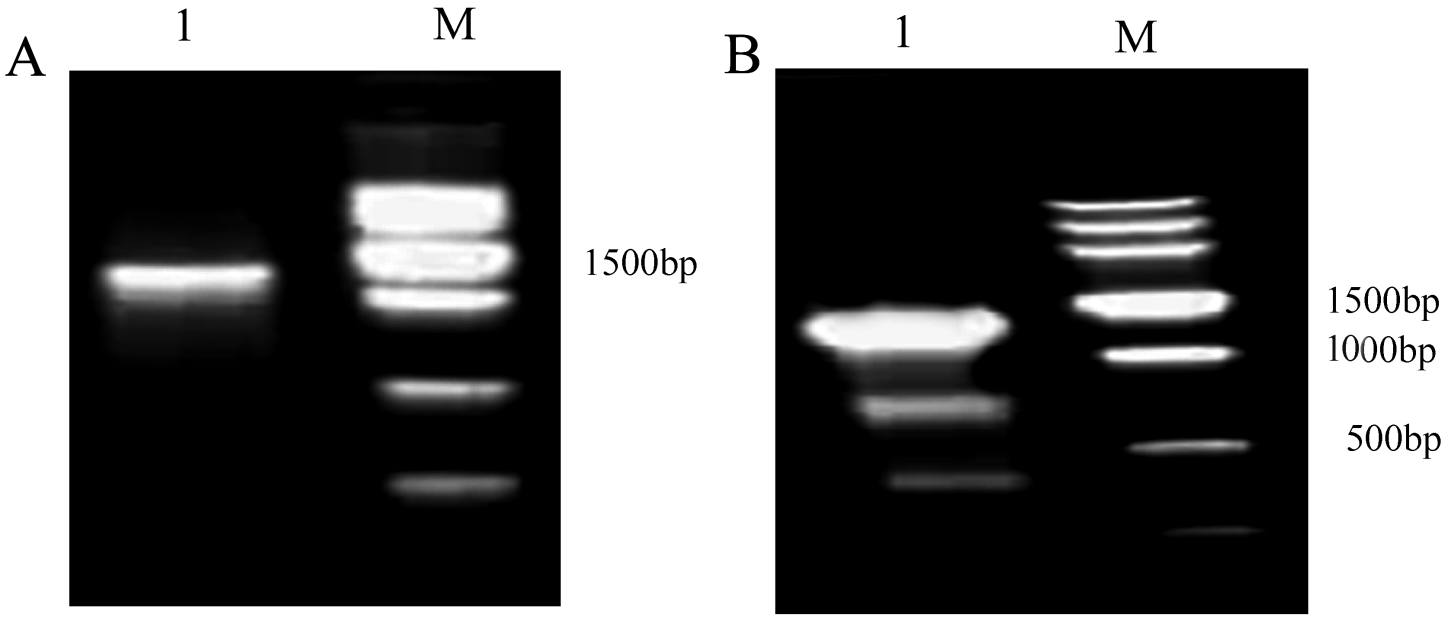

Figure 1

Gel electrophotogram of 5' and 3' RACE products of the CDS2 gene. A. 5' RACE; and B. 3' RACE. 1, RACE products; M, marker.

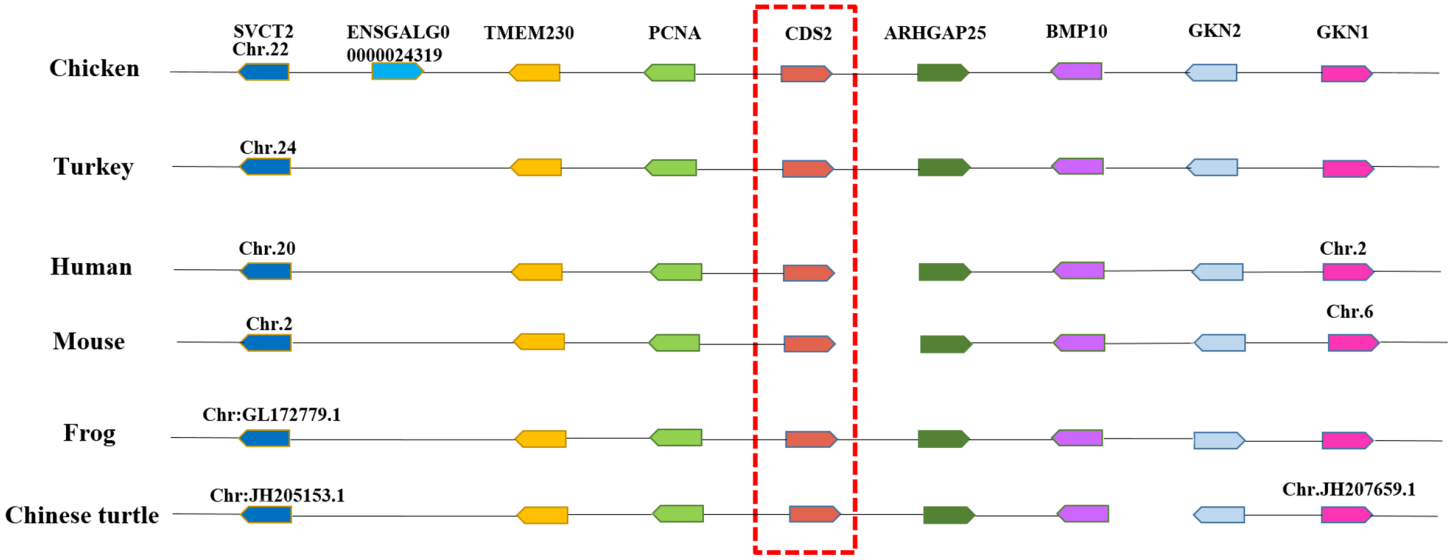

Figure 2

Gene arrangement of the genomic region encompassing CDS2. Boxes in the same column with the same color represent homologous genes in the corresponding species. Arrows represent the direction of transcription of genes.

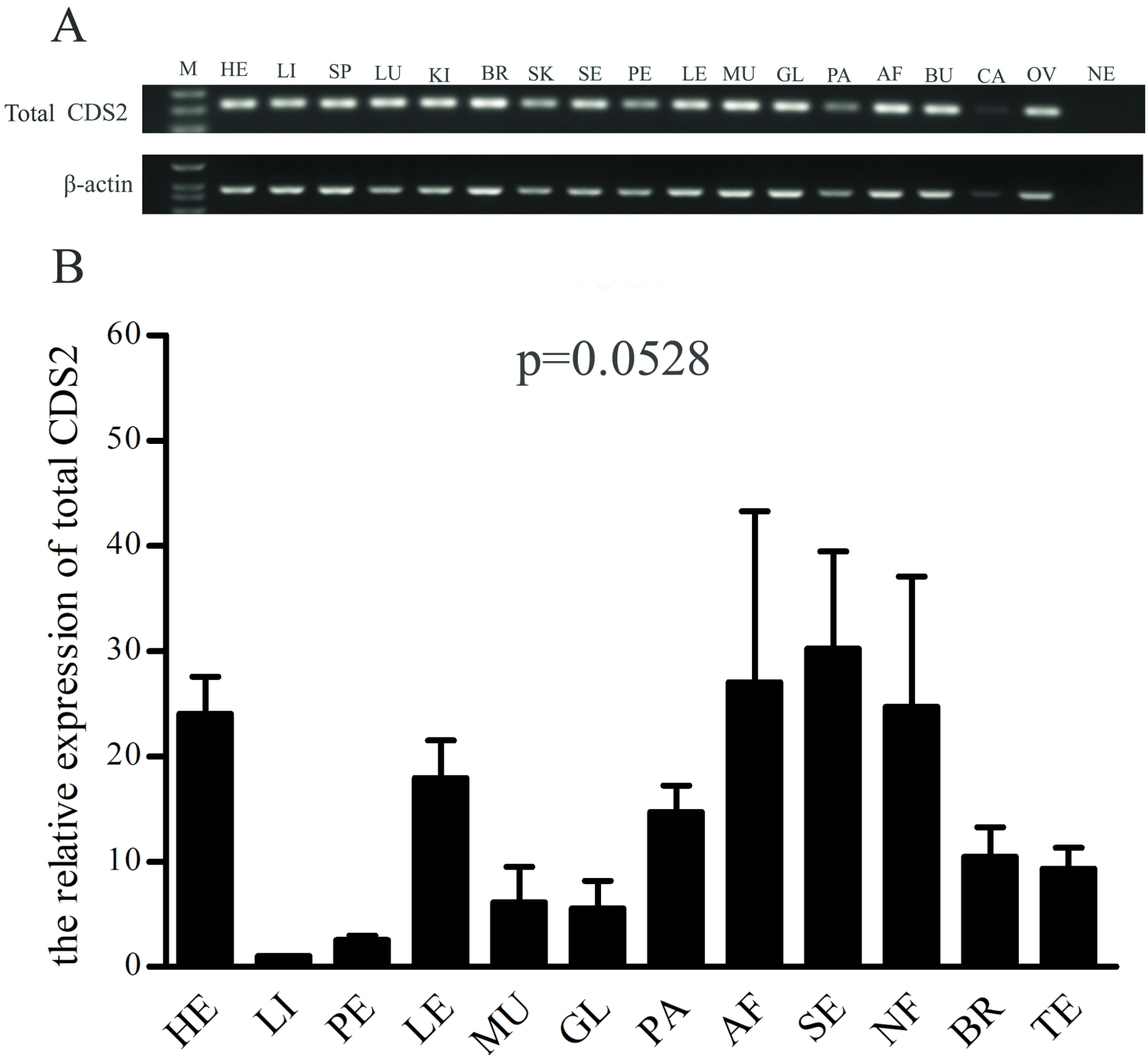

Figure 3

Tissue expression profile of chicken total CDS2. A. mRNA level of total CDS2 detected by semi-quantitative RT-PCR (female); B. mRNA level of total CDS2 detected by qPCR (n = 3, male). The β-actin gene was used as an internal control. Abbreviations: HE, heart; LI, liver; SP, spleen; LU, lung; KI, kidney; BR, brain; SK, skin; AF, abdominal fat; SE, sebum; NE, neck fat; PE, pectoralis; LE, leg muscle; MU, muscular stomach; GL, glandular stomach; PA, pancreas; BU, bursa of Fabricius; CA, cartilage; OV, ovary; TE, testis; NE, negative control; M, DNA marker (DL 700).

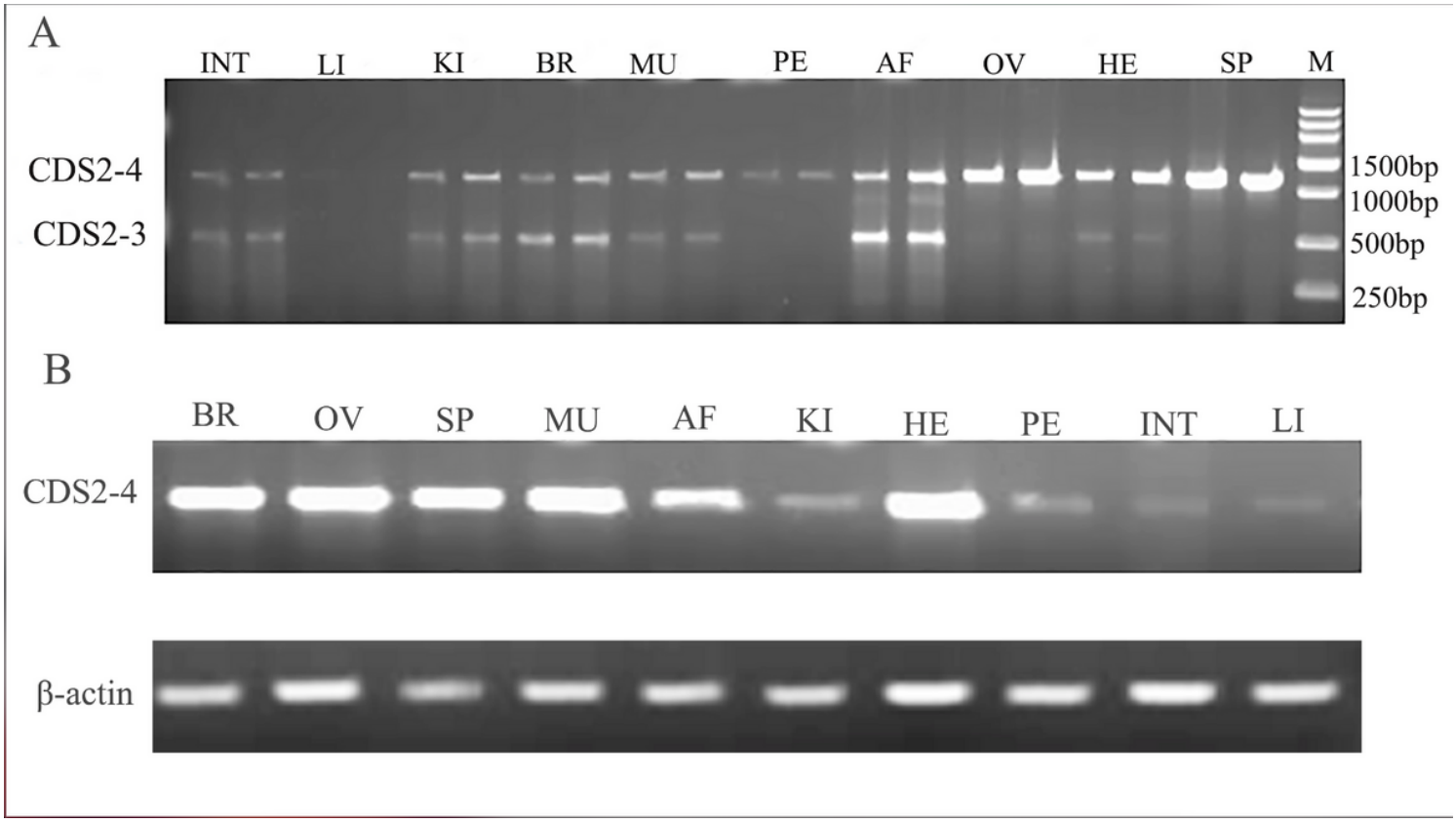

Figure 4

Tissue expression pattern of CDS2 detected by RT-PCR with AS1 and QP2 primer sets. A. AS1 PCR products; B. QP2 PCR products. The β-actin gene was used as an internal control. Abbreviations: INT, small intestine; LI, liver; KI, kidney; BR, brain; MU, muscular stomach; PE, pectoralis; AF, abdominal fat; OV, ovary; HE, heart; SP, spleen.

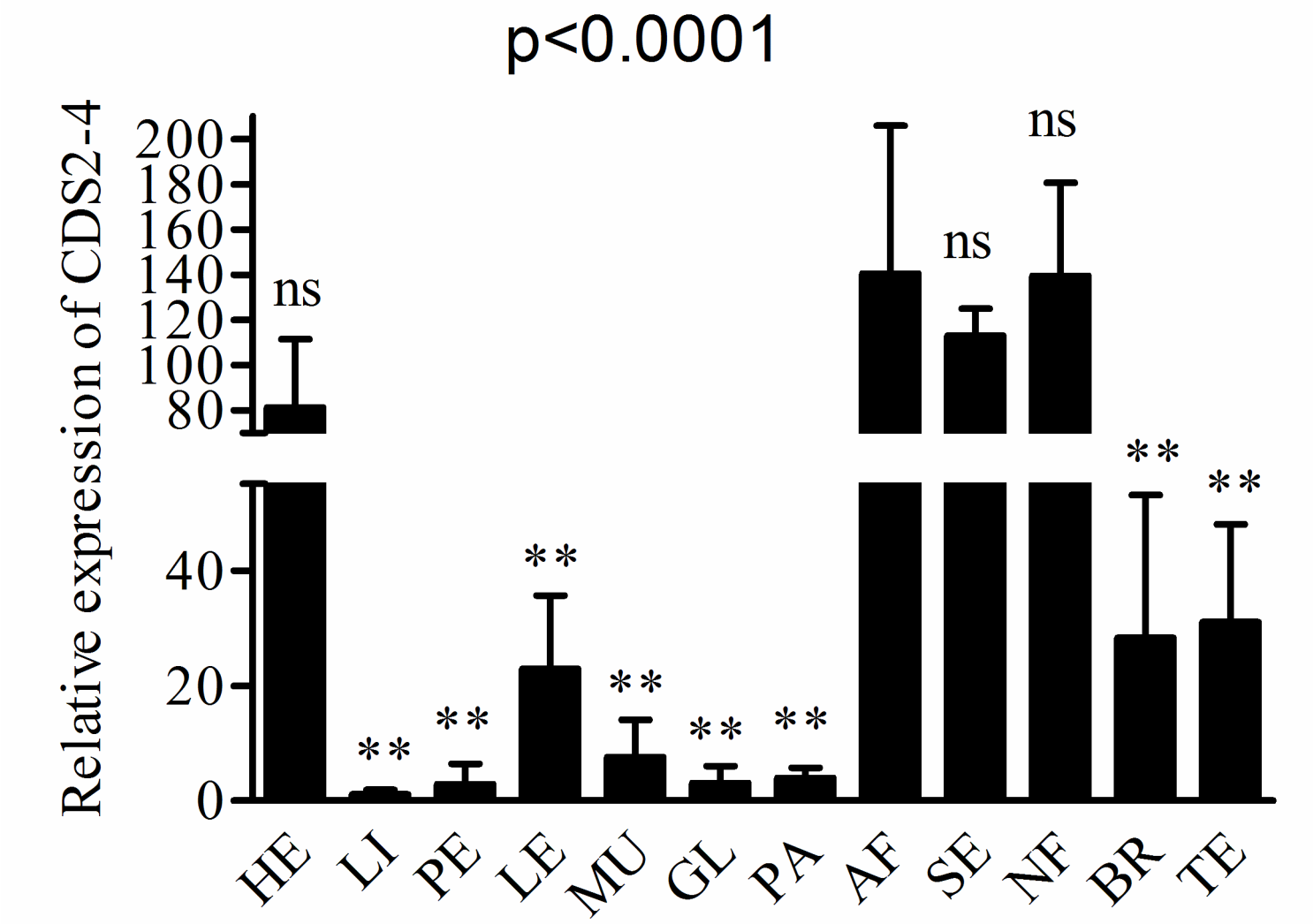

Figure 5

Tissue expression profile of chicken CDS2-4 detected by qPCR (n = 3, male). Pair comparison was conducted using the Bonferroni method with AF as a control. **, P < 0.01; ns, p > 0.05. Abbreviations: HE, heart; LI, liver; PE, pectoralis; LE, leg muscle; MU, muscular stomach; GL, glandular stomach; PA, pancreas; AF, abdominal fat; SE, sebum; NE, neck fat; BR, brain; TE, testis.

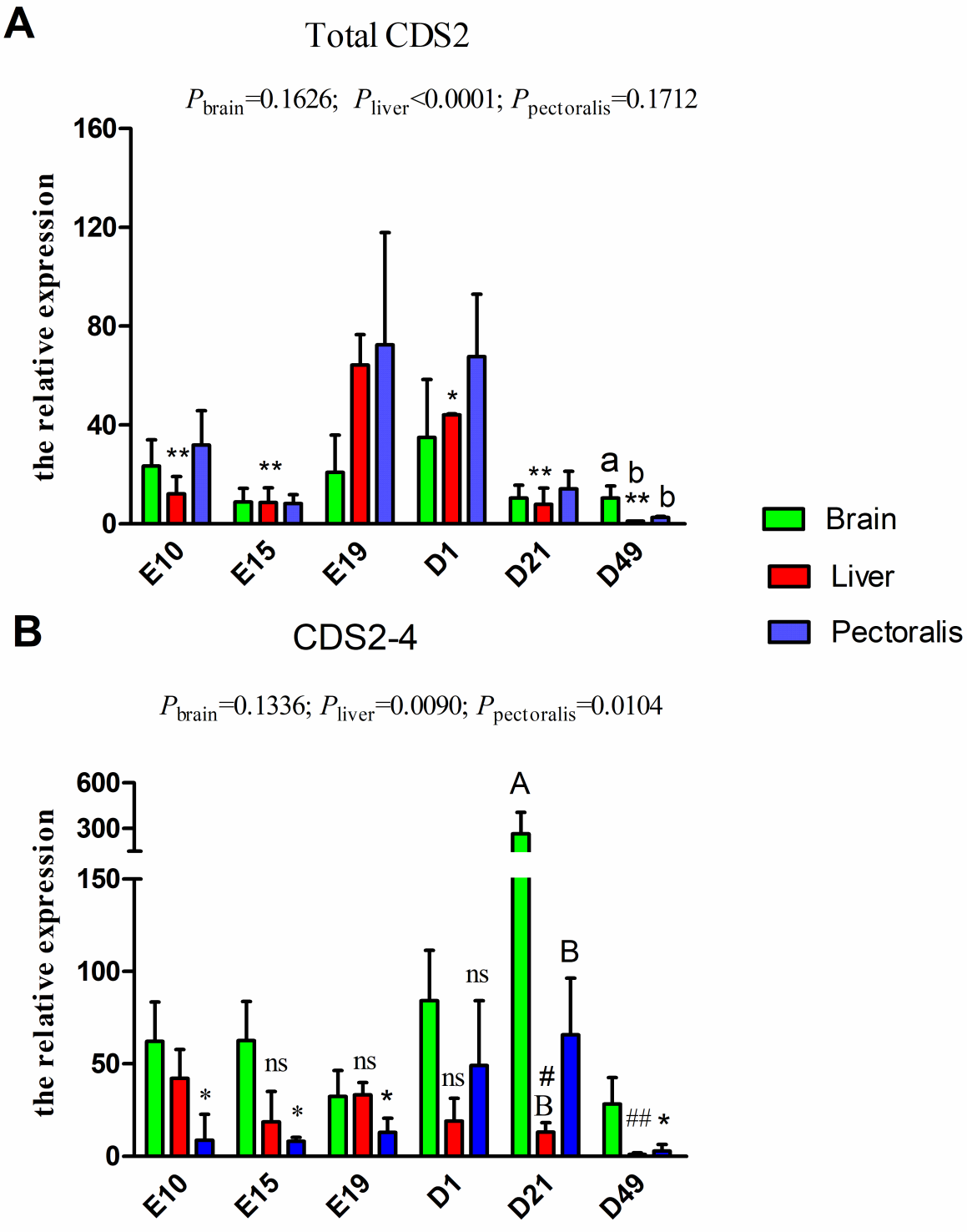

Figure 6

Spatio-temporal expression pattern of total CDS2 and CDS2-4. Pairwise comparison was conducted using the Bonferroni method in tissues with P < 0.05, where the time point with the highest value was taken as a control. * and #, P < 0.05; ** and ##, P < 0.01; ns, P > 0.05. Different lowercase letters indicate P < 0.05; different uppercase letters indicate P < 0.01, and no symbol indicates P > 0.05. A. Total CDS2

with E19 as a control in the liver. B. CDS2-4 with E10 as a control in the liver, and D21 as a control in the pectoralis.

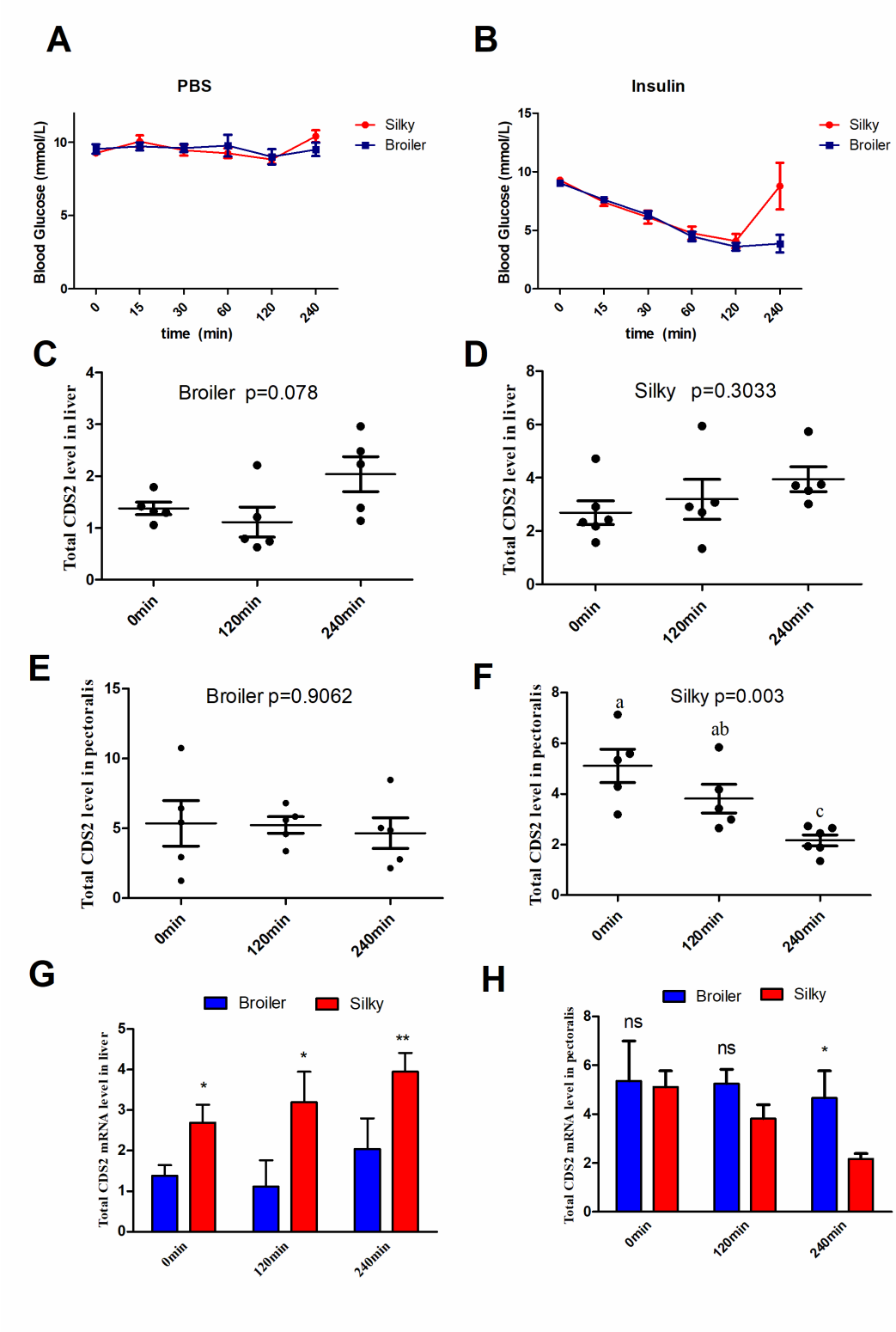

Figure 7

Effect of insulin on blood glucose and mRNA levels of total CDS2. A. Blood glucose in PBS control. B. Blood glucose after insulin treatment (80 μg/kg body weight). C. Total CDS2 in liver of broilers. D. Total CDS2 in liver of Silky chickens. E. Total CDS2 in pectoralis of broilers. F. Total CDS2 in pectoralis of Silky

chickens; G. Total CDS2 in liver. H. total CDS2 in pectoralis. C–F, different letters indicate $P < 0.05$, no letter or same letter indicates $P > 0.05$. In G and H, data were only compared between two breeds at the same time point. *, $P < 0.05$; ns, $P > 0.05$. Data are presented are mean ± standard error.

Supplementary Files

This is a list of supplementary files associated with this preprint. Click to download.

- SuppmentaryTable.docx
- 1.pdf
- 2.pdf
- 3.pdf
- Fig.S4.tif